Reconstruction of Ob River, Russia, discharge from ring widths of floodplain trees

Article · October 2016

CITATIONS
2

READS
93

3 authors:

Leonid Agafonov
Russian Academy of Sciences
24 PUBLICATIONS **113** CITATIONS
SEE PROFILE

David M. Meko
The University of Arizona
120 PUBLICATIONS **7,210** CITATIONS
SEE PROFILE

Irina P. Panyushkina
The University of Arizona
74 PUBLICATIONS **311** CITATIONS
SEE PROFILE

Journal of Hydrology 543 (2016) 198–207

Contents lists available at ScienceDirect

Journal of Hydrology

journal homepage: www.elsevier.com/locate/jhydrol

Research papers

Reconstruction of Ob River, Russia, discharge from ring widths of floodplain trees

Leonid I. Agafonov [a], David M. Meko [b,*], Irina P. Panyushkina [b]

[a] Institute of Plant and Animal Ecology UB RAS, 202 Marta 8th St., Yekaterinburg 620144, Russia
[b] Laboratory of Tree-Ring Research, University of Arizona, 1215 E. Lowell St., Tucson, AZ 85721, USA

ARTICLE INFO

Article history:
Received 3 June 2016
Received in revised form 3 August 2016
Accepted 10 September 2016
Available online 13 September 2016
This manuscript was handled by K. Georgakakos, Editor-in-Chief

Keywords:
Dendrohydrology
Ob River
Streamflow reconstruction
Tree rings
Arctic Ocean warming
Northern Eurasia river discharge variability

ABSTRACT

The Ob is the third largest Eurasian river supplying heat and freshwater to the Arctic Ocean. These inputs influence water salinity, ice coverage, ocean temperatures and ocean circulation, and ultimately the global climate system. Variability of Ob River flow on long time scales is poorly understood, however, because gaged flow records are short. Eleven tree-ring width chronologies of *Pinus sibirica* and *Larix sibirica* are developed from the floodplain of the Lower Ob River, analyzed for hydroclimatic signal and applied as predictors in a regression model to reconstruct 8-month average (December-July) discharge of the Ob River at Salekhard over the interval 1705–2012 (308 yrs). Correlation analysis suggests the signal for discharge comes through air temperature: high discharge and floodplain water levels favor cool growing-season air temperature, which limits tree growth for the sampled species at these high latitudes. The reconstruction model (R^2 = 0.31, 1937–2009 calibration period) is strongly supported by cross-validation and analysis of residuals. Correlation of observed with reconstructed discharge improves with smoothing. The long-term reconstruction correlates significantly with a previous Ob River reconstruction from ring widths of trees outside the Ob River floodplain and extends that record by another century. Results suggest that large multi-decadal swings in discharge have occurred at irregular intervals, that variations in the 20th and 21st centuries have been within the envelope of natural variability of the past 3 centuries, and that discharge data for 1937–2009 underestimate both the variability and persistence of discharge in the last 3 centuries. The reconstruction gives ecologists, climatologists and water resource planners a long-term context for assessment of climate change impacts.

1. Introduction

Much attention has been paid to research on river runoff in the context of global climate change (ACIA, 2005; Serreze et al., 2006; IPCC, 2013; Harding et al., 2011). Such attention is deserved because river runoff is an important component of the hydrological cycle and a main constituent of the climate system. Terrestrial water-cycle processes regulating evaporation, runoff and changes in the hydrological cycle are directly linked with atmospheric processes (Chahine, 1992; Rawlins et al., 2010; Shiklomanov et al., 2011; Polyakov et al., 2013). The terrestrial hydrological cycle is especially important for the Arctic Ocean "where the volume of sea water is relatively small as compared with the volume of river water entering the ocean" (Shiklomanov and Shiklomanov, 2003). Changes in the terrestrial hydrologic budget of the Northern Hemisphere influence the freshwater inflow to the Arctic Ocean (Peterson et al., 2002, 2006; McClelland et al., 2004; Mauritzen, 2012), which in turn affects ocean salinity, sea-ice coverage, and ocean circulation (Aagaard and Carmack, 1989; Polyakov et al., 2013). Annual river discharge comprises 38% of the freshwater input to the Arctic Ocean (Serreze et al., 2006), and the export of river freshwater to the Arctic Ocean is about 11% of the global river discharge (Shiklomanov, 2000).

The degree to which discharge of Arctic rivers is affected by climate change is as yet speculative. Peterson et al. (2006) suggest that the river discharge correlates with changes in both the North Atlantic Oscillation and global mean surface air temperature. They note the average annual rate of river discharge from 6 major Eurasian rivers increased at about 2.0 ± 0.7 $km^3\ yr^{-1}$ from 1936 to 1999 and is greater now (about 128 $km^3\ yr^{-1}$) than it was in the 1930s (Peterson et al., 2002). The most obvious change in northern Eurasia river discharge is an increase in winter flows (Peterson et al., 2002; Shiklomanov and Shiklomanov, 2003; Yang et al., 2004; Rennermalm et al., 2010).

* Corresponding author.
E-mail addresses: lagafonov@ipae.uran.ru (L.I. Agafonov), dmeko@LTRR.arizona.edu (D.M. Meko), ipanyush@email.arizona.edu (I.P. Panyushkina).

http://dx.doi.org/10.1016/j.jhydrol.2016.09.031
0022-1694/

A credible reason for this mode of change is the impact of dams built for generation of hydroelectric power (McClelland et al., 2004; Magritskii, 2008; Adam et al., 2007). Another possible reason is a rise of air temperature in autumn over the basins and an associated delayed establishment of snow cover (Barnett et al., 2005; Agafonov, 2010). One point of view is that recent increasing river discharge in Eurasia is a fluctuation rather than a change. Early studies identified cycles at wavelength ~25–30 years in river discharge and lake levels over Inner Eurasia (Shnitnikov, 1968). More recently researchers argue that the "interannual variation of the total river runoff into the Arctic Ocean and the total runoff of the Asian rivers into the ocean over the historical period of observations is statistically homogeneous with a clearly defined quasi-periodicity " (Simonov and Khristoforov, 2005).

Understanding the discharge variability of rivers flowing into the Arctic Ocean is important not only to address to the impact of climate change, but also to improve water and natural resources management across the drainage basins. Tree-ring records are a valuable proxy for extending the historical observations of runoff (Meko and Woodhouse, 2011). MacDonald et al. (2007) applied the Eurasian network of tree-ring sites to reconstruct 200 years of regional variability in discharge of seven major Eurasian rivers flowing into the Arctic Ocean. The reconstructions showed no significant upward trend in annual discharge during the 20th Century, and suggested that discharge variations during that century were within bounds of the natural variability at longer time scales. Among the rivers reconstructed by MacDonald et al. (2007) was the Ob, whose annual discharge accounts 8% of the total freshwater inflow to the Arctic (Lammers et al., 2001). In this study we suggest a new approach to reconstruct Ob River discharge that exploits the temperature sensitivity of tree rings of floodplain trees. Tree growth of conifers along the Lower Ob is strongly limited by air temperature and reflects water level fluctuations. High water levels and floods cool down surface air temperature over the floodplain and reduce radial growth of trees (Agafonov and Mazepa, 2001). Conversely, low water levels link to warmer air temperatures and higher tree-ring growth. The Ob River generates a local climate characterized by air temperature anomalies related to water level. A marked air temperature gradient exists away from the river bed, such that the observed increase in air temperature can reach 0.5–1.5 °C at a distance of 500 m from the river bed (Vendrov, 1970).

We sampled tree rings of *Pinus sibirica* and *Larix sibirica* along the Lower Ob to test the hydrological signal in ring width using linear regression and the gaged discharge at Salekhard, near the mouth of the Ob. The goal was to reconstruct Ob River discharge for a period greater than 200 years and to evaluate short-term and long-term variability of discharge in the context of previous dendrohydrological studies.

2. Study area

The Ob River and its major tributary, the Irtysh, (combined length 3650 km, drainage area 2,972,497 km^2) are located in western Siberia (Fig. 1). From snow-dominated headwaters in the Altay-Sayan Mountain belt of Inner Asia, the Ob flows into the Arctic Ocean through the Kara Sea. The Ob River has the largest watershed of all Arctic rivers and the third largest runoff after the Yenisey and Lena Rivers (SWC, 1984). Mean annual discharge of the Ob at Salekhard, 70 km from the mouth of the river, is

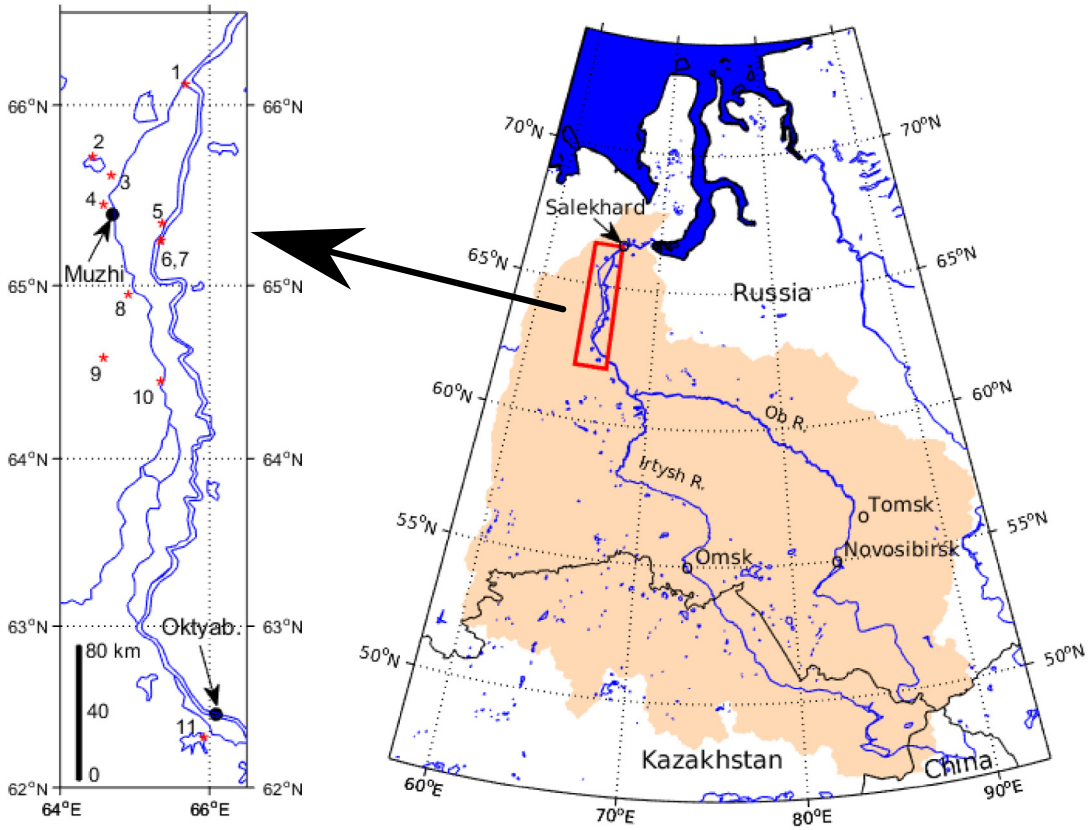

Fig. 1. Map of study area. Inset shows locations of 11 tree-ring sites numbered as in Table 2. Headwaters of the Ob River main stem are in Russia. The headwaters of the Irtysh River are in Kazakhstan and China. Tree-ring sites are along lower Ob River. Gaged flow record reconstructed is at Salekhard, upstream of the mouth of the Ob River where it enters the Kara Sea. Muzhi and Oktyabrskoe (inset map) are rural settlements with precipitation and temperature records used in correlation analysis.

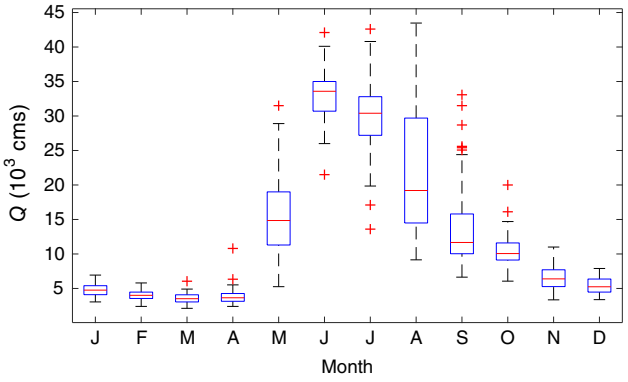

Fig. 2. Mean monthly hydrograph of Ob River at Salekhard. Analysis period 1936–2009. Distributions for individual months are displayed as box plots with a horizontal line at the median, a box over the interquartile range, and plus signs at values more than 1.5 times the interquartile range above or below the box. If there are no such outliers, the brackets mark the data extremes.

12,475 m^3/s or 394 km^3/yr (ArcticRIMS). Approximately 70% of the Ob's annual discharge occurs during the ice-free period from May to October, and 80% of the annual runoff originates southward of 61°N latitude, which is about 1150 km from the Ob estuary (SWC, 1984). The hydrological regime of the Ob River is dominated by snowmelt, with peak flows in June-July (Fig. 2). The maximum discharge usually occurs in June because of snowmelt floods (Yang et al., 2004). Summer precipitation contributes to the high August runoff, which varies greatly from one year to another. Precipitation in the Ob River catchment is driven by disturbances in the westerlies, and the hydroclimatic regime is influenced by interactions between the Siberian High and westerly jet stream over the Eurasian continent (Panagiotopoulos et al., 2005).

Several major hydropower dams, built beginning in the 1950s, are located above the confluence of the Ob and Irtysh (McClelland et al., 2004). Reservoir operations have demonstrably changed the seasonality of river flows in the Ob Basin. The primary measurable effect has been an increase in winter flows and a decrease in summer flows (Yang et al., 2004). Water use by agriculture and the metal industry in the relatively densely populated Middle Ob region has also impacted the seasonal variability of flows south of the confluence with the Irtysh River (Yang et al., 2004). The Lower Ob River – north of the confluence - has neither major dams and reservoirs nor high-density population.

This study sampled tree rings from trees growing on the floodplain along a 500 km reach of the Lower Ob River (Fig. 1). The Lower Ob River floodplain covers area of about 20×10^3 km^2. The flat topography of the West Siberian Plains accommodates a floodplain with a width ranging from 20 km to 60 km. This area is prone to extensive summer inundation that can last for several months. During episodes of large inundation the Lower Ob floodplain is capable of storing more than 100 km^3 of water (Antipov and Bachurin, 1989). Such storage can be expected to modify air surface temperatures as energy from radiation is directed to latent heat rather than sensible heat.

3. Data and methods

3.1. Hydroclimatic data

Monthly data of Ob River discharge for the gage at Salekhard (N66°32′, E66°36′) was downloaded from the ArcticRIMs database (http://rims.unh.edu). The gaged record at Salekhard begins in 1936 and has been used in various hydrologic studies to represent the variability of freshwater contribution of the Ob River to the Arctic Ocean (e.g., Lammers et al., 2001; Yang et al., 2004; Adam et al., 2007). The Salekhard gage data is part of the Regional Arctic Hydrographic Network, or R-ArcticNET v.2.2, a set of more than 3000 recording stations defining contemporary hydrography of the pan-Arctic lands. The data were digitized from original hydrological yearbooks by the R-ArcticNET group and have been screened for quality control through calculation of gridded runoff surfaces for the Arctic region (Lammers et al., 2001). The Salekhard gage is a certified station of the Federal Service for Hydrometeorology and Environmental Monitoring of Russia (Roshydromet). The observation system at Salekhard is typical of Eurasian stations that use horizontal-axis current meters. Water-level records are read off a pile, with a base water level at a height of 0.44 m above sea level (Baltic system). The location of the gage and methodology of discharge measurement have not to our knowledge changed over the operation period. Typical errors for measured discharge are in the range of ±2–5% for non-ice conditions in such rivers with floodplains (Rantz et al., 1982; Russian Hydro Meteorological Service, 1970). Winter discharge measurements under ice conditions are less accurate, with the potential errors of 15–30% over the Arctic regions (Grabs et al., 2000).

Discharge for the water year (October-September) over the 73 years 1937–2009 is slightly autocorrelated at a lag of 1 year ($r1 = 0.35$), and varies greatly from year to year – from 29% below the long-term mean to 44% above the mean (Table 1). Relationships between the tree-ring data and climate were summarized using monthly precipitation and temperature data from the RIHMI database (www.meteo.ru) for stations Muzhi and Oktyabrskoye. A monthly climogram for Muzhi illustrates the strongly continental climate regime along the Low Ob (Fig. 3). Monthly precipitation typically peaks in mid-summer. The growing season, defined by monthly mean temperatures above 0 °C, is May-September. This monthly growing season can be considerably extended in some years, as evidence by occasional means above freezing for April and October (Fig. 3).

3.2. Tree-ring data

Two cores per tree (13–47 trees) were sampled from six sites of *Larix sibirica* and five sites of *Pinus sibirica* on the floodplain of the Lower Ob (Fig. 1, Table 2). The sampled trees are from riverbanks less than 400 m away from the main channel or from terraces no more than 30 m above the water level (Table S1). The sampled trees themselves are upland as opposed to riparian, and are not subject to damage or inundation by annual flooding. While some

Table 1
Discharge statistics[a] of Ob River at Salekhard, 1936–2009.

Season	Mean	Median	Std. Dev.	r_1	Min%	Max%
June	32,887	33,584	3450	0.17	65	128
October	10,373	10,060	2238	0	58	193
Water Year	12,769	12,683	12,683	0.35	71	144
December-July	12,545	12,492	12,492	0.23	76	122

[a] Mean, median and standard deviation in m^3/s; lag-1 autocorrelation (r_1), and minimum and maximum values as percentage of mean.

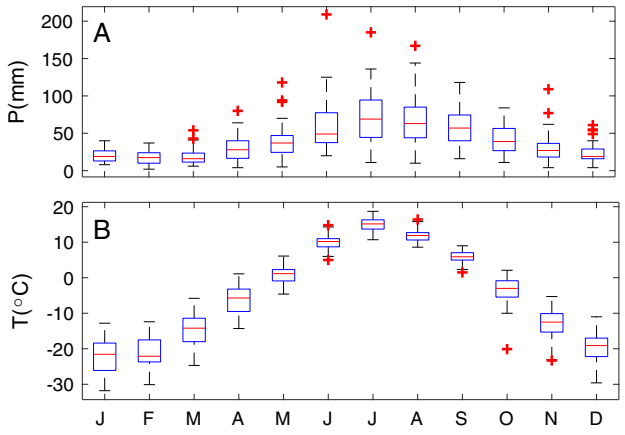

Fig. 3. Climogram from station Muzhi, Russia. (A) Monthly precipitation, 1932–1988. (B) Monthly mean temperature, 1932–1990. Distributions of monthly data are summarized by boxplots, as defined in the caption to Fig. 2. The mean annual precipitation at Muzhi is 479 mm, and the mean annual temperature is −4.7 °C.

sites were first sampled as early as 1990, all were updated by the authors during major sampling campaigns in 2012–2014. Samples were prepared and rings dated and measured by conventional methods (Stokes and Smiley, 1996). Cross-dating and measurements were checked with program COFECHA (Holmes, 1983) and site chronologies were generated with program ARSTAN (Cook et al., 2007). Each chronology was prepared with the same protocol: (1) fit each ring-width series with a cubic smoothing spline with a frequency response of 0.5 at a wavelength 2/3 the sample length (Cook and Peters, 1981), (2) remove trend by taking the ratio of measured widths to the fitted line, (3) combine index series for individual cores using a bi-weight robust mean (Cook and Kairiukstis, 1990), and (4) variance-stabilize the resulting site chronology to adjust for time-varying sample size (Osborn et al., 1997). Adequacy of the sample size to capture the population signal for tree-ring variation at the site was assessed with the expressed population signal (EPS; Wigley et al., 1984).

3.3. Reconstruction and analysis

Site chronologies were transformed by principal components analysis (PCA; Mardia et al., 1979) into orthogonal variables for possible use as predictors in reconstruction models. This approach has been widely used in dendrohydrologic reconstruction to reduce redundancy in tree-ring data (e.g., Meko et al., 2001, 2007; Woodhouse et al., 2006). PCA was run on the correlation matrix of the 11 site chronologies for their 1705–2012 common period, and the important components were identified using an eigenvalue-of-1 rule and scree plot (Mardia et al., 1979).

The seasonal climatic signal in tree-ring series was identified with program Seascorr (Meko et al., 2011), which examines correlations and partial correlations between a tree-ring series and climatic data aggregated over variable-length seasons.

The season for discharge reconstruction was selected by stepwise regression (Weisberg, 1985) of Ob River at Salekhard discharge (monthly or seasonal), 1937–2009, on the tree-ring PC time series. We used gaged discharge, rather than discharge adjusted for upstream anthropogenic influences (dams, changes in water usage, etc.) because our sampled trees are downstream of the reservoirs. Variations in air temperature directly influencing the growth of the sampled trees according to our conceptual model are driven by variations in actual rather than adjusted flows. Tree-growth at the sampled sites as well as reconstructed discharge will consequently reflect the combination of natural and anthropogenic factors influencing discharge and water levels along the lower Ob River. Trial regressions were run, each time varying the ending month and length of season for average discharge. Stepwise entry of predictors in model trials was guided by *p*-to-enter and *p*-to-remove thresholds of 0.05 and 0.10 (Weisberg, 1985). Cross-validation (Michaelsen, 1987) was done at each step as a safeguard against model over-fitting, such that an additional step in the stepwise procedure was accepted only if that step yielded an increase in skill as measured by the reduction-of-error statistic (RE; Cook and Kairiukstis, 1990).

The regression model for the optimal season, as identified above, was then re-calibrated, subjected to analysis of residuals to identify possible violations of regression assumptions (Weisberg, 1985), and applied to the extended record of tree-ring PC scores to generate a long-term reconstruction of discharge, 1705–2012. A confidence interval around the reconstruction was estimated from the cross-validation mean-square error of the regression and the assumption that the reconstruction errors are normally distributed. Extrapolations, or reconstructed values for years in which the predictors are outside the multivariate space they occupy in the calibration period, were identified by the ellipsoid method described by Weisberg (1985, p. 236).

Linear relationships between pairs of time series were described by the Pearson correlation coefficient (Haan, 2002), with significance level adjusted as needed to account for autocorrelation in time series as suggested by Dawdy and Matalas (1964). Low frequency variations in time series were extracted by Gaussian filters designed with specific cutoff frequencies (Mitchell et al., 1966). "Discrete" peaks or troughs (highs or lows) in smoothed series were defined as those separated by more than the width

Table 2
Tree-ring site locations and statistics.

#	Site ID[a]	N Lat.	E Lon.	Sample size[b] N_T/N_c	Span & critical year[c]	Ob River Corr.[d]
1	LV	66° 05	65° 41	35/57	1662–2013 (1745)	−0.41
2	LL	65° 41	64° 26	47/82	1539–2013 (1590*)	−0.39
3	KV	65° 35	64° 42	35/55	1559–2012 (1635*)	−0.44
4	LPU	65° 25	64° 35	19/25	1671–2013 (1695)	−0.39
5	LP	65° 19	65° 23	34/53	1555–2014 (1635)	−0.45
6	LLG	65° 13	65° 21	13/18	1665–2014 (1720)	−0.38
7	KLG	65° 13	65° 21	30/47	1535–2014 (1590)	−0.40
8	KU	64° 55	64° 55	34/56	1420–2013 (1555)	−0.38
9	KL	64° 33	64° 35	44/64	1599–2013 (1700)	−0.40
10	KK	64° 25	65° 21	19/24	1705–2012 (1760)	−0.19
11	LT	62° 17	65° 56	37/49	1566–2014 (1600*)	−0.35

[a] Site ID: first letter L = *Larix sibirica* (Siberian larch) and K = *Pinus sibirica* (Siberian pine).
[b] Number of trees (N_T) and number of cores (N_c).
[c] First and last year of data, with first year that EPS > 0.85 in parentheses; asterisk = first available year for EPS estimate.
[d] Correlation of tree-ring series with discharge (Dec-July average) over 1937–2009.

of the corresponding Gaussian filter used for smoothing. Weights of filters used in this paper are listed in the Supplementary Material.

Simple linear regression (variable against time) was applied to test for trend in time series; a slope coefficient differing from zero at a specified α-level by a *t*-test was accepted as evidence of significant linear trend. Periodicity was tested by the smoothed periodogram method of spectral analysis (Bloomfield, 2000). For an appropriate "simultaneous" confidence interval on the spectrum, the theoretical interval based on a chi-square distribution was widened to account for multiple tests using Bernoulli's inequalities (Snedecor and Cochran, 1989, p. 116).

4. Results and discussion

4.1. Hydrologic signal in tree rings

PCA on the 11 standard tree-ring chronologies, 1705–2012, indicated that the primary mode of variation is same-sign growth departure at all sites. This common-growth mode is summarized by PC1, which accounts for 54% of the tree-ring variance (Table 3). While eigenvalues exceed 1.0 for only the first two PCs, a scree plot suggests four PCs (85% cumulative variance) should be retained for subsequent analysis (Fig. S2). PC2 is a species contrast, with opposite-sign loading on larch and pine. PC3 is a regional contrast, with negative loadings on just the southernmost 3 sites. PC4 is more complex than the other PCs, but its main contrast is a far-north larch site (LV, #1 in Fig. 1) with a far-south pine site (KK, #10 in Fig. 1).

Table 3
Site loadings of first four principal components[a] of 11 tree-ring chronologies.

Site ID	PC1	PC2	PC3	PC4
LV	0.2627	−0.3763	0.0436	0.5533
LL	0.3163	−0.3297	0.1764	−0.1339
KV	0.3432	0.1795	0.1744	0.1076
LPU	0.3418	−0.2325	0.0657	−0.2232
LP	0.3223	−0.3052	0.051	−0.0518
LLG	0.3264	−0.2387	0.0501	−0.3122
KLG	0.2928	0.3759	0.0201	0.3115
KU	0.317	0.3158	0.0255	0.1597
KL	0.3189	0.3388	−0.0306	0.1924
KK	0.2542	0.3837	−0.0427	−0.5954
LT	0.1829	−0.1012	−0.9609	0.0168

[a] PCA was done on the correlation matrix of the 1705–2012 matrix of chronologies; cumulative percentage of variance explained by 4 PCs is 85%; individual percentages are 54%, 20%, 7% and 4%.

Seascorr results for tree-ring PC1 with the Muzhi monthly and seasonal climatic observations show that tree-growth is positively correlated with air temperature in the warm season (Fig. 4, top). Partial correlations (controlling for temperature) show additional positive contribution to growth from high precipitation in June (Fig. 4, bottom). Previous studies have indicated the importance of a few weeks in June and July to cambial activity and tree-ring formation at such high-latitude locations in Siberia (Vaganov et al., 2006; Rossi et al., 2008). The positive temperature correlation is consistent with other studies showing that tree-growth of the sampled species at this high-latitude location is limited by low temperature (Vaganov et al., 1996). We hypothesize that the positive correlation of growth to June precipitation reflects the importance of soil moisture in facilitating or hindering the transfer of heat from the air to the root system of the trees: high June precipitation and a wet soil profile favor heat transfer into the soil when June air temperature is high.

The relationship between air temperature and tree-growth is critical to the reconstruction of Ob River discharge from floodplain trees along the Lower Ob. Ob River discharge at Salekhard closely tracks Ob water levels throughout the Lower Ob River Basin (Agafonov and Mazepa, 2001), and water level variations from year to year are negatively correlated with air temperatures at the tree-ring sites (Table 2). Relationships can be summarized with the discharge record at Salekhard and climate data from Muzhi. Positive correlation between these variables through the ice-free cool-season months reaches peak significance ($p < 0.001$) in May, and then switches abruptly to a weakly significant ($p < 0.05$) negative correlation in June (Fig. 5). This pattern of correlation is consistent with the water from the south warming the normally cool air during the cooler months of the year and moderating the warm air temperature during the late spring and early summer. As tree-growth for the species used here does not normally begin until June (Agafonov and Gurskaya, 2013), the dominant indirect river

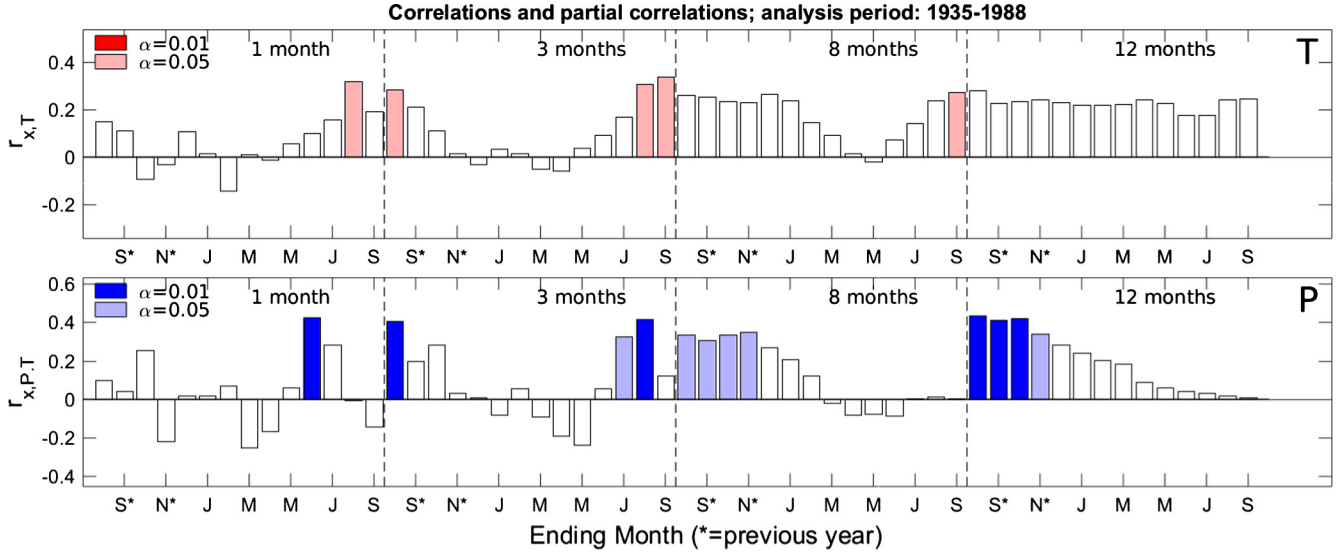

Fig. 4. Monthly and seasonal correlations of tree-ring PC1 with climate data for Muzhi. Output from program Seascorr shows correlations of PC1 with temperature (T-top) and partial correlations with precipitation (P-bottom). Results shown for "seasons" of length 1, 3, 8 and 12 months with variable ending month. Significance estimated by Monte Carlo method (Meko et al., 2011) is color coded for two α levels.

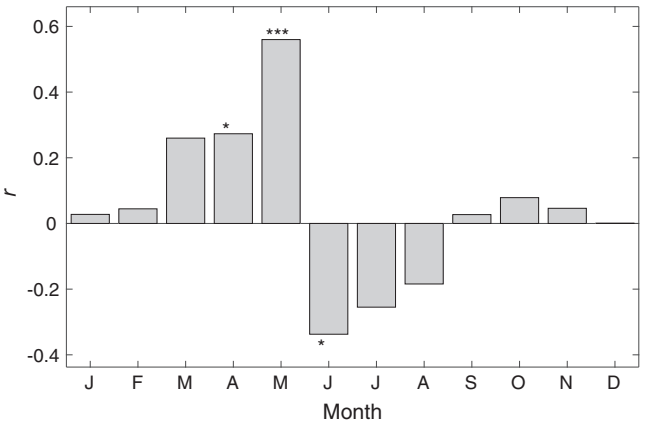

Fig. 5. Bar chart of correlations of monthly discharge of Ob River with monthly mean air temperature at Muzhi. Station Muzhy is in the floodplain of the Ob near the largest group of tree-ring sites. Discharge is for gage at Salekhard. Analysis period 1936–1990. Significance at <0.05, <0.01, and <0.001 marked by 1, 2, or 3 asterisks. Sample size for assessing significance is reduced to account for significant autocorrelation in the individual series, following Dawdy and Matalas (1964). At most this adjustment in any month is to 48 years from the full sample size of 55 years.

influence on tree growth is to reduce growth in high-flow years and increase growth in low-flow years.

Stepwise regression of discharge at Salekhard on PCs 1–4 of tree rings for various seasonal groupings of discharge ending with July of the growth year indicates maximum strength of signal ($R^2 = 0.31$, $F = 15.6$, $p < 1E{-}5$) for an 8-month window beginning in December preceding the growth year (Fig. 6). The signal, while much weaker than that for some basins in temperate latitudes, such as the Sacramento (Meko et al., 2001) and Colorado (Woodhouse et al., 2006), was judged strong enough to justify a reconstruction effort.

4.2. Streamflow reconstruction

The reconstructed model selected from the exploratory stepwise regression just described and calibrated on the years 1937–2009, is

$$\hat{y} = \hat{a} + \hat{b}_1 x_1 + \hat{b}_2 x_2,$$

where x_1 and x_2 are scores of PCs 1 and 4, respectively, of the 11 tree-ring chronologies; $\hat{a}$, $\hat{b}_1$, and $\hat{b}_2$ are the estimated regression constant and coefficients; and $\hat{y}$ is the reconstructed discharge

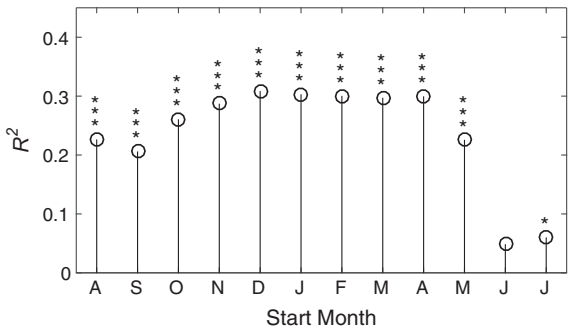

Fig. 6. Seasonal variability of strength of tree-ring signal for discharge. Strength measured by R^2 for stepwise regression model of discharge averaged over various periods ending with July of the growth year on PCs 1–4 of tree rings. Significance of overall F-level of equation indicated by 3, 2, or 1 asterisks ($p < 0.001$, $p < 0.01$, $p < 0.05$).

Table 4
Statistics[a] of stepwise regression for reconstruction model.[b]

Step	Predictors	R^2	R^2 adj.	RE	p_{DW}
1	PC1	0.24	0.23	0.18	0.29
2	PC1, PC4	0.31	0.29	0.24	0.79

[a] For each step, the regression R^2, adjusted R^2, reduction-of-error statistic, and p-value of Durbin-Watson test for lag-1 autocorrelation of residuals.

[b] Equation of reconstruction model is Q = 12599.8731 -728.9757 PC1 -367.699 PC4, where Q is Dec-July average discharge in m^3/s, and predictors PC1 and PC4 are z-scores (scaled by 1937–2009 means and standard deviations) of tree-ring principal components.

(December-July average). Positive cross-validation RE indicates skill of reconstruction using data not used in calibration (Table 4). No appreciable gain in RE resulted from letting additional PCs enter as predictors into the model. An analysis of residuals indicated no obvious problems, such as non-normality of residuals or systematic dependence of variance of residuals on fitted (reconstructed) discharge (Figs. S3 and S4). In particular, the null hypothesis of non-autocorrelated residuals could not be rejected based on the Durbin-Watson statistic (Table 4). For a long-term reconstruction, the PC scores (PCs 1 and 4) for the period 1705–2012 were substituted into the reconstruction equation. A 1705 start year was supported by the statistical summary of the tree-ring data, which indicated that the EPS threshold of 0.85 was reached before 1705 at most sites, and as early as 1555 at one site (Table 2).

The reconstruction tracks observed discharge at annual and decadal time scales during the calibration period (Fig. 7). As expected with such a low regression R^2, large discrepancies occur in some years – e.g., the failure to identify low discharge in 1954 and 1967. The largest negative and positive reconstruction errors (1967 and 1973) happen to occur in years with relatively low June precipitation. This finding is consistent with our hypothesis of a dry June soil profile opposing a strong growth response to air temperature variations. Field studies and multi-year time series of vertical profiles of soil moisture and temperature, are needed, however, to rigorously test the hypothesis. Reconstruction bias in discharge statistics for the calibration period includes underestimation of lag-1 autocorrelation and large underestimation of spread – a necessary consequence of regression $R^2 \ll 1$ (Table 5). The bias dictates using the reconstructed discharge alone (i.e., rows 2 vs 3 in Table 5) for a long-term context of short-period discharge statistics. The reconstruction viewed in this way suggests that the snapshot for1937–2009 underestimates both the variability (standard deviation and range) and lag-1 autocorrelation of discharge of the past 300 years.

4.3. Analysis of reconstruction

Reconstructed discharge, 1705–2012, varies greatly at high and low frequencies, and has its high and low extremes before the start of the gaged record, in 1937 (Fig. 8). Uncertainty is summarized by the 50% confidence interval: the true (unknown) discharge in any given year has a 50% chance of falling outside the displayed confidence interval. Years flagged as extrapolations in Fig. 8 have additional uncertainty, as the predictors (PC1 and PC4) in those years fall outside an ellipse describing the bivariate domain of the predictors in the calibration period. Eight extrapolations occur in the long-term reconstruction.

While the annual reconstruction leaves 69% of variance of discharge over the calibration period unexplained, accuracy is improved with smoothing (Fig. 9). For example, the correlation of observed with reconstructed discharge increases from $r = 0.55$ for the unsmoothed reconstruction to $r = 0.69$ for the reconstruction smoothed with a 10-year Gaussian filter. Accordingly, we assess

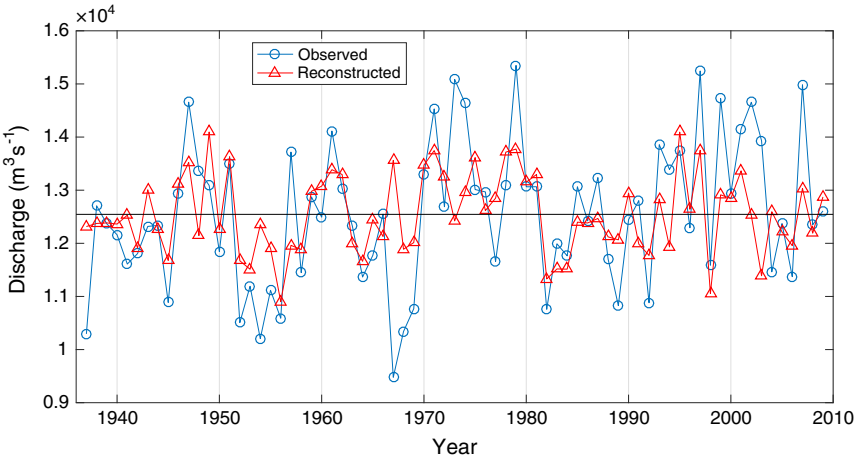

Fig. 7. Time plots of observed and reconstructed discharge for 1937–2009 calibration period of reconstruction model. Horizontal line at calibration-period mean.

Table 5
Statistics[a] of observed and reconstructed discharge of Ob River at Salekhard.

Season	Mean	Median	Std. Dev.	r_1	Min%	Max%
Observed	12,545	12,492	1343	0.23	76	122
Rec: 1937–2009	12,545	12,422	746	0.11	87	112
Rec: 1705–2012	12,600	12,588	854	0.35	81	120

[a] Mean, median and standard deviation in m^3/s; lag-1 (year) autocorrelation; and maximum and minimum as percentage of observed mean.

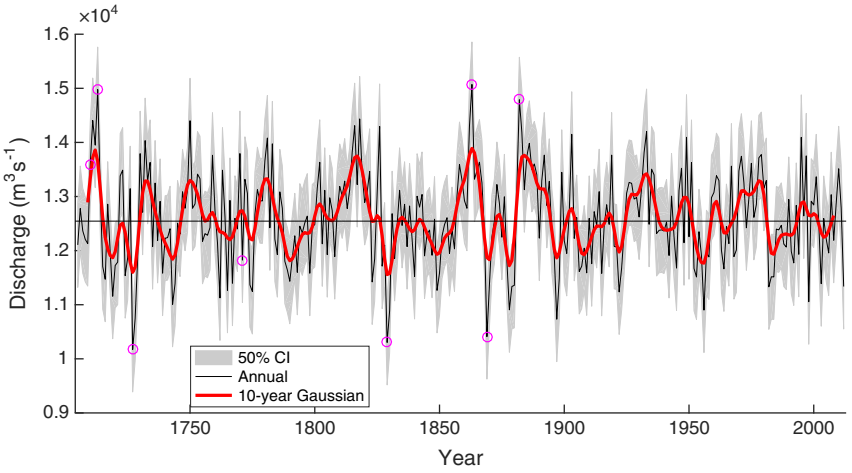

Fig. 8. Time plot of reconstructed discharge of Ob River at Salekhard, 1705–2012. Confidence interval (50%) applies to the unsmoothed reconstruction, which is an annual series of discharge averaged over December-July. Decadal variations are emphasized by Gaussian smoothing (red line). Horizontal line at 12,545 m^3/s marks the mean for the 1937–2009 calibration period. Magenta circles mark the 8 reconstruction years classified as extrapolations. (For interpretation of the references to colour in this figure legend, the reader is referred to the web version of this article.)

dry periods and wet periods by lows and highs in the reconstruction after smoothing. The 10-year Gaussian smoothed series is plotted in Fig. 8, while lows and highs the unsmoothed reconstruction and at three levels of smoothing are listed in Table 6. For 10-year smoothing, reconstructed lows in 1727, 1829 and 1878 are below the reconstructed extreme calibration period reconstructed low of 11,769 m^3/s, in 1956. Seven discrete peaks in the 10-yr smoothed series before 1937 are higher than the highest calibration-period peak, in 1978. Multi-decadal periods of relatively low and high variability recur in different parts of the series. Most prominent are two wet intervals in the latter half of the 19th century. Annual and smoothed reconstructions both suggest the gaged period (1937–2009) underestimates the range of natural variability of discharge.

While spline detrending as applied here in chronology development would remove any climatic trend at wavelengths on the order of the length of individual measured ring-width series or longer (Cook et al., 1995), shorter trends will be retained in the reconstruction. Trends persisting over 2–3 decades are evident in the reconstruction (Fig. 8). Significant trend is found over the 1937–2009 calibration for the gaged discharge, but not for the reconstruction (Fig. 7). As a percentage of the mean per decade this recent trend,

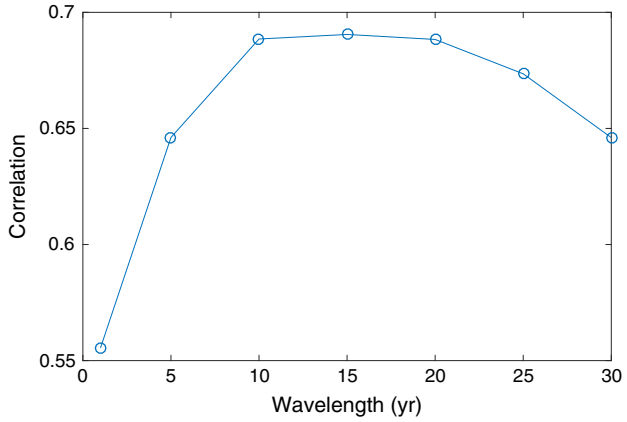

Fig. 9. Correlation of observed with reconstructed discharge as a function of smoothing. Leftmost point is for the unsmoothed series ($R^2 = 0.31$, or $r = 0.55$). Other points are for series smoothed with successively broader Gaussian filters, with 50% frequency response at 5, 10, 15, 20, 25 and 30 years.

Table 6
Lows and highs in annual and smoothed reconstructed discharge.

		Extremes[b] (10^2 m^3/s)		
	W[a] (yr)	1937–2009	1705–1936	N[c]
Lows	1	109	102	6
	5	114	110	5
	10	118	116	3
	20	121	120	4
Highs	1	141	151	12
	5	136	144	7
	10	133	139	7
	20	131	135	4

[a] Extreme reconstructed discharge in calibration period (1937–2009) and prior to start of calibration period (1705–1936).
[b] W = wavelength of 50% amplitude response of Gaussian filter used to smooth series ("1" indicates unsmoothed series).
[c] Number of discrete (see Data and Methods) lows or highs in 1705–1936 more extreme than any in 1937–2009.

with significance in parentheses, is $\Delta Q = 1.38\%$ $(p = 0.02)$ for the gaged discharge and $\Delta Q = 0.08\%$ $(p = 0.81)$ for the reconstruction. The trend in gaged discharge is consistent with the general tendencies (see Introduction) for the Arctic rivers in Eurasia. The discrepancy in recent trend between gaged and reconstructed discharge is reflected in a significant positive trend in regression residuals of the reconstruction model (Fig. S4). The trend in gaged December-July discharge is driven primarily by trend in winter discharge, when trees are dormant and relatively insensitive to variation in air temperature variations and discharge (Fig. S7).

The time plot of reconstructed discharge in Fig. 8 is characterized by high-amplitude multi-decade swings of potential importance to water and power management on the Ob, as well as to ecology of the basin. Spectral analysis does not, however, support significant periodicity in the annual reconstruction (Fig. S5). No spectral peaks are significant at $\alpha = 0.01$, even without widening the confidence interval around the spectrum to account for multiple comparisons. The smooth decadal fluctuations in the reconstructed discharge can be best described as irregular.

Only one previous Ob River reconstruction, by MacDonald et al. (2007) exists for comparison with our new reconstruction. For brevity, we abbreviate the reconstructions here as "M2007" and "A2016". The two reconstructions are independent in that M2007 is based on a large Eurasian network of tree-ring chronologies, none of which are in A2016, and none of which are along the Low Ob River. The conceptual model for M2007 relies on spatial anomalies in tree-ring growth on a continental scale capturing synoptic climatological variability (e.g., ridges, troughs, storm tracks) related to runoff, while our model relies on a local response of trees along the Lower Ob River to air temperature variation specifically driven by water levels on the Ob. The predictand for both reconstructions is discharge at Salekhard, but for M2007 is "adjusted" discharge for the water year, and for A2016 is unadjusted discharge averaged for December-July.

Despite the aforementioned differences, the two reconstructions share many features (Fig. 10), and are significantly correlated over their 1800–1990 common period ($r = 0.53$, $p < 0.001$; Fig. S6). For neither reconstruction are the discharge fluctuations in the 20th century outside the range of natural variability estimated by tree rings. The new reconstruction suggests that this finding could be modified to include the first decade of the 21st century (Fig. 8). A caveat to this conclusion is that the fluctuations in discharge sensed by the trees since the 1950s may be somewhat damped by effects of reservoir operation upstream. Reservoir operations on the Ob River have been associated with increasing winter flows and decreasing summer flows in the middle and upper Ob valleys (Yang et al., 2004). No quantitative assessment is available on the net effect on the flood coverage along the Lower Ob River following spring ice break. While the total maximum capacity of reservoirs is only 15% of the mean annual discharge of the Ob at Salekhard (Yang et al., 2004), some reservoir effect on lower Ob

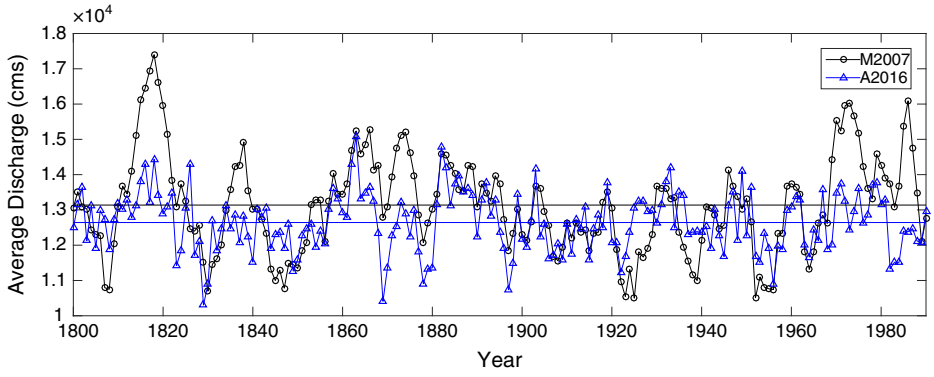

Fig. 10. Reconstructed discharge of Ob River at Salekhard by two tree-ring studies. A2016 is from current study, and is December-July average. M2007 is from MacDonald et al. (2007), and is October-September average. A2016 and M2007 also differ in that A2016 is gaged discharge, while M2007 is discharge series adjusted for reservoir operations and other anthropogenic factors. The two respective 1800–1990 means (horizontal lines) are 13,138 m^3/s and 12,642 m^3/s. The two series correlate strongly over their full overlap, 1800–1990 ($r = 0.55$, $p < 0.001$).

flood coverage during the growing season of the trees used in this study is likely.

5. Conclusions and perspective

The main finding of this study is that useful information on long-term variability of Ob River discharge can be obtained from ring widths of conifers growing on banks and fluvial terraces along lower reaches of the river. The discharge signal depends on the combination of temperature sensitivity of tree growth, seasonality of tree-ring formation, and large-scale modification of floodplain air temperatures by inter-annual water-level variations of the river. According to our conceptual model, high Ob River discharge measured at Salekhard coincides with greater surface water storage and water coverage in the lower Ob Basin, lower air temperatures, and reduced tree growth. Conversely low Ob River discharge is associated with warmer air temperatures and increased tree growth. June precipitation may modulate the tree-growth response to temperature through soil moisture variation during a critical period of ring formation: wet soils facilitate heat transfer and vice versa. A 308-year reconstruction of discharge based on this signal suggests that large, irregular, fluctuations in discharge on decadal and multi-decadal time scales are characteristic of the Ob River, and that recent fluctuations have been exceeded in amplitude by fluctuations before the start of gaged discharge record.

Future studies should attempt to combine the type of discharge signal illustrated here with other tree-ring information for improved accuracy of reconstruction of discharge of the Ob River and possibly of other large northern rivers. That only 31% of the variance of December-July discharge can be reconstructed from our tree-ring network underscores the fact that tree growth along the Lower Ob is imperfectly related to air temperature and that air temperature is imperfectly related to water level fluctuation of the Ob River. Large-scale tree-ring networks, such as that used by MacDonald et al. (2007) could possibly be used adjust for influence other than Ob water levels on air temperatures in the lower basin. For example such networks might be able to identify episodes of temperature advection during the growth season of the trees due to anomalous positioning of ridges and troughs.

While the sampled trees for this study are from slightly elevated settings not subject to inundation for periods of weeks to months, extensive stands of riparian trees that can tolerate inundation can also be found along the Lower Ob River. Such trees could be investigated for complementary tree-ring information on discharge using ring-width patterns (e.g., Meko et al., 2015) or morphological features of the annual rings (e.g., St. George, 2010; Therrell and Bialecki, 2015).

Acknowledgements

This work was supported by grants from the CRDF Global Research Partnerships program (#RUC1-7075-EK-12 and #FSCX-15-61824-0), and Russian Foundation for Basic Research (#13-04-01964, #05-04-48298, #00-05-65041). We acknowledge also the generous assistance in provision of a research vessel and land facilities by the Institute of Plant and Animal Ecology, Ural Branch of Russian Academy of Sciences, in Yekaterinburg and Labytnangi.

Appendix A. Supplementary material

Supplementary data associated with this article can be found, in the online version, at http://dx.doi.org/10.1016/j.jhydrol.2016.09.031.

References

Aagaard, K., Carmack, E.C., 1989. The role of sea ice and other fresh water in the Arctic circulation. J. Geophys. Res. 94 (C10), 14485–141498.
ACIA, 2005. Arctic Climate Impact Assessment. Cambridge Univ. Press, Cambridge. 1042 pp.
Adam, J.C., Haddeland, I., Su, F., Lettenmaier, D.P., 2007. Simulation of reservoir influences on annual and seasonal streamflow changes for the Lena, Yenisei, and Ob' rivers. J. Geophys. Res. 112 (D2411). http://dx.doi.org/10.1029/2007JD008525.
Agafonov, L.I., Mazepa, V.S., 2001. Runoff of Ob River and summer air temperature in the north of Western Siberia. Proc. Russ. Acad. Sci.: Geograph. Ser. (Izvestiya AN. Seriya Geographicheskaya) 1, 82–90.
Agafonov, L.I., 2010. Change of Lower Ob River discharge in the XX century. Proc. Russ. Acad. Sci.: Geograph. Ser. (*Izvestiya RAN: Seriya Geographicheskaya*) 4, 68–76.
Agafonov, L.I., Gurskaya, M.A., 2013. Influence of the Lower Ob River flow on tree ring growth. Contem. Prob. Ecol. 6 (7), 779–787.
Antipov, A.N., Bachurin, G.B. (Eds.), 1989. Landscape and Hydrology of Western Siberia. SB RAN Institute of Geography, Irkutsk. 222 pp.
Barnett, T.P., Adam, J.C., Lettenmaier, D.P., 2005. Potential impacts of a warming climate on water availability in snow-dominated regions. Nature 438, 303–309.
Bloomfield, P., 2000. Fourier Analysis of Time Series: An Introduction. John Wiley & Sons, New York. 261 pp.
Chahine, M.T., 1992. The hydrological cycle and its influence on climate. Nature 359, 374–380.
Cook, E.R., Peters, K., 1981. The smoothing spline: a new approach to standardizing forest interior tree-ring width series for dendroclimatic studies. Tree-Ring Bullet. 41, 45–53.
Cook, E.R., Kairiukstis, L.A. (Eds.), 1990. Methods of Dendrochronology: Applications in the Environmental Sciences. Kluwer Academic Publishers, Dordrecht. 394 pp.
Cook, E.R., Briffa, K.R., Meko, D.M., Funkhouser, G., 1995. The "segment length curse" in long tree-ring chronology development for paleoclimatic studies. The Holocene 5 (2), 229–237.
Cook, E.R., Krusic, P.J., Holmes, R.H., Peters, K., 2007. Program ARSTAN, Version 41d, 2007 <www.ldeo.columbia.edu/tree-ring-laboratory>.
Dawdy, D.R., Matalas, N.C., 1964. Statistical and probability analysis of hydrologic data, part III analysis of variance, covariance and time series. In: Chow, V.T. (Ed.), Handbook of Applied Hydrology: A Compendium of Water-Resources Technology. McGraw-Hill Book Company, New York, pp. 8.69–8.90. 1440 pp.
Grabs, W.E., Fortmann, F., Couet, T.D., 2000. Discharge observation networks in Arctic regions: computation of the river runoff into the Arctic Ocean, its seasonality and variability. In: Lewis, E.L. et al. (Eds.), Freshwater Budget of the Arctic Ocean. Kluwer Academic, pp. 249–268.
Haan, C.T., 2002. Statistical Methods in Hydrology. Iowa State University Press. 496 pp.
Harding, R., Best, M., Blyth, E., Hagemann, S., Kabat, P., Tallaksen, L.M., Warnaars, T., Wiberg, D., Weedon, G.P., van Lanen, G., Ludwig, F., Haddeland, I., 2011. WATCH: current knowledge of the terrestrial global water cycle. J. Hydrometeorol. 12, 1149–1156.
Holmes, R.L., 1983. Computer-assisted quality control in tree-ring dating and measurement. Tree Ring Bull. 43, 69–78.
IPCC, 2013. Climate change 2013: The physical science basis. In: Stocker, T.F., Qin, D., Plattner, G.-K., Tignor, M., Allen, S.K., Boschung, J., Nauels, A., Xia, Y., Bex, V., Midgley, P.M. (Eds.), Contribution of Working Group I to the Fifth Assessment Report of the Intergovernmental Panel on Climate Change. Cambridge University Press, Cambridge, United Kingdom and New York, USA. 1535 pp.
Lammers, R.B., Shiklomanov, A.I., Vörösmarty, C.J., Fekete, B.M., Peterson, B.J., 2001. Assessment of contemporary Arctic river runoff based on observational discharge records. J. Geophys. Res. 106, 3321–3334.
MacDonald, G.M., Kremenetski, K.V., Smith, L.C., Hidalgo, H.G., 2007. Recent Eurasian river discharge to the Arctic Ocean in the context of longer-term dendrohydrological records. J. Geophys. Res-Biogeo 112 (G4). http://dx.doi.org/10.1029/2006JG000333.
Magritskii, D.V., 2008. Anthropogenic impact on the runoff of Russian rivers emptying into the Arctic Ocean. Water Resour. 35 (1), 1–14 [original Russian Text © D.V. Magritskii, 2008, published in Vodnye Resursy, 2008, Vol. 35, No. 1, pp. 3–16].
Mardia, K., Kent, J., Bibby, J., 1979. Multivariate Analysis. Academic Press, London. 518 pp.
Mauritzen, C., 2012. Arctic freshwater. Nat. Geosci. 5, 163–165.
McClelland, J.W., Holmes, R.M., Peterson, B.J., Stieglitz, M., 2004. Increasing river discharge in the Eurasian Arctic: consideration of dams, permafrost thaw, and fires as potential agents of change. J. Geophys. Res. 109, D18102. http://dx.doi.org/10.1029/2004JD004583.
Meko, D.M., Therrell, M.D., Baisan, C.H., Hughes, M.K., 2001. Sacramento River flow reconstructed to A.D. 869 from tree rings. J. Am. Water Resour. Assoc. 37 (4), 1029–1040.
Meko, D.M., Woodhouse, C.A., Baisan, C.A., Knight, T., Lukas, J.J., Hughes, M.K., Salzer, M.W., 2007. Medieval drought in the Upper Colorado River Basin. Geophys. Res. Lett. 34 (L10705). http://dx.doi.org/10.1029/2007GL029,988.
Meko, D.M., Touchan, R., Anchukaitis, K.A., 2011. Seascorr: a MATLAB program for identifying the seasonal climate signal in an annual tree-ring time series. Comput. Geosci. 37, 1234–1241.
Meko, D.M., Woodhouse, C.A., 2011. Application of streamflow reconstruction to water resources management. In: Hughes, M.K., Swetnam, T.W., Diaz, H.F.

(Eds.), Dendroclimatology. Progress and Prospects, Developments in Paleoenvironmental Research, vol. 11. Springer, Netherlands, pp. 231–261.
Meko, D.M., Friedman, J.M., Touchan, R., Edmondson, J.R., Griffin, E.R., Scott, J.A., 2015. Alternative standardization approaches to improving streamflow reconstructions with ring-width indices of riparian trees. The Holocene 25 (7), 1093–1101. http://dx.doi.org/10.1177/0959683615580181.
Michaelsen, J., 1987. Cross-validation in statistical climate forecast models. J. Clim. Appl. Meteor. 26, 1589–1600.
Mitchell, J.M. Jr, Dzerdzeevskii, B., Flohn, H., Hofmeyr, W.L., Lamb, H.H., Rao, K.N., Walléen, C.C., 1966. Climatic change. Technical Note 79, Report of a working group of the Commission for Climatology 195 TP 100, WMO, Geneva, Switzerland, 81 pp.
Osborn, T.J., Briffa, K.R., Jones, P.D., 1997. Adjusting variance for sample-size in tree-ring chronologies and other regional mean time series. Dendrochronologia 15, 89–99.
Panagiotopoulos, F., Shahgedanova, M., Hannachi, A., Stephenson, D., 2005. Observed trends and teleconnections of the Siberian High. J. Clim. 18, 1411–1422.
Peterson, B.J., Holmes, R.M., McClelland, J.W., Vörösmarty, C.J., Lammers, R.B., Shiklomanov, A.I., Shiklomanov, I.A., Rahmstorf, S., 2002. Increasing river discharge to the Arctic Ocean. Science 298, 2171–2173. http://dx.doi.org/10.1126/science.
Peterson, B.J., McClelland, J.W., Curry, R., Holmes, R.M., Walsh, J.E., Aagaard, K., 2006. Trajectory shifts in the Arctic and Subarctic freshwater cycle. Science 313, 1061–1066.
Polyakov, I.V., Bhatt, U.S., Walsh, J.E., Abrahamsen, E.P., Pnyushkov, A.V., Wassmann, P.F., 2013. Recent oceanic changes in the Arctic in the context of long-term observations. Ecol. Applicat. 23 (8), 1745–1764.
Rantz, S.E., Barnes H.H., Kilpatrick, F.A., Carter,R.W., Cobb, E.D., Smoot, G.F., Benson, M.A., Matthai, H.F., Dalrymple, T., Pendleton, J.A.F., Kindsvater, C.E., Hulsing, H., Tracy, H.J., Bodhaine, G.L., Wilson, J.F., Davidian, J., 1982. Measurement and Computation of Streamflow: Volume 1. Measurement of Stage and Discharge, Geological Survey Water Supply Paper 2175, Unites States Government Printing Office, Washington, D.C., 284 pp.
Rawlins, M.A., Steele, M., Holland, M.M., 2010. Analysis of the Arctic system for freshwater cycle intensification: observations and expectations. J. Clim. 23, 5715–5737.
Rennermalm, A.K., Wood, E.F., Troy, T.J., 2010. Observed changes in pan-arctic cold-season minimum monthly river discharge. Clim. Dyn. 35, 923–939.
Rossi, S., Deslauriers, A., Griçar, J., Seo, J.-W., Rathgeber, C.B.K., Anfodillo, T., Morin, H., Levanic, T., Oven, P., Jalkanen, R., 2008. Critical temperatures for xylogenesis in conifers of cold climates. Glob. Ecol. Biogeogr. 17, 696–707.
Russian Hydrometeorological Service, 1970. Observations on USSR Hydrometeorological Network: Determination of Hydrometeorological Elements and Observations Occurrence Estimates (In Russia). Gidrometeoizdat, St. Petersburg.
Serreze, M.C., Barrett, A.P., Slater, A.G., Woodgate, R.A., Aagaard, K., Lammers, R.B., Steele, M., Moritz, R., Meredith, M., Lee, C.M., 2006. The large-scale freshwater cycle of the Arctic. J. Geophys. Res. 111, C11010. http://dx.doi.org/10.1029/2005JC003424.
Shiklomanov, I.A., 2000. Appraisal and assessment of world water resources. Water Int. 25 (1), 11–32.
Shiklomanov, A.I., Shiklomanov, I.A., 2003. Climatic change and the dynamics of river runoff into the Arctic Ocean. Water Resour. 30 (6), 593–601.
Shiklomanov, A.I., Bohn, T.J., Lettenmaier, D.P., Lammers, R.B., Romanov, P., Rawlins, M.A., Adam, J.C., 2011. Interactions between land cover/use change and hydrology. In: Gutman, G., Reissell, A. (Eds.), Eurasian Arctic Land Cover and Land Use in a Changing Climate. Springer, Dordrecht.
Shnitnikov, A.V., 1968. Multidecadal Variability of Surface Water. Nauka, Leningrad. 246 pp.
Simonov, Yu.A., Khristoforov, A.V., 2005. Analysis of many-year variations of runoff in river runoff into the Arctic Ocean. Water Resour. 32 (6), 587–593.
Snedecor, G.W., Cochran, W.G., 1989. Statistic Methods. Iowa State University Press. 503 pp.
SWC, 1984. State Water Cadastre. Data on Hydrological Regime and Water Resources, vol. 1. Issue 10, Gidrometeoizdat, Leningrad, 320 pp.
St. George, S., 2010. Tree rings as paleoflood and paleostage indicators. In: Stoffel, M., Bollschweiler, M., Butler, D.R., Luckman, B.H. (Eds.), Tree-Ring Reconstructions in Natural Hazards Research: A State-of-the-Art Advances in Global Change Research Series. Springer, New York, pp. 233–240.
Stokes, M.A., Smiley, T.L., 1996. An Introduction to Tree-Ring Dating. University of Arizona Press, Tucson (originally published 1968, University of Chicago Press), 73 pp.
Therrell, M.D., Bialecki, M.B., 2015. A multi-century tree-ring record of spring flooding on the Mississippi River. J. Hydrol. 529, 490–498.
Vaganov, E.A., Shiyatov, S.G., Mazepa, V.S., 1996. Dendroclimatic Studies in the Ural-Siberian Subarctic. Nauka, Novosibirsk. 244 pp.
Vaganov, E.A., Hughes, M.K., Shashkin, A.V., 2006. Growth Dynamics of Conifer Tree Rings: Images of Past and Future Environments. Springer-Verlag, Berlin, Heidelberg. 343 pp.
Vendrov, T., 1970. Impact of Reservoirs of the Forest Zone on Surrounding Areas (in Russian). Science Publishing House, Moscow. 220 pp.
Weisberg, S., 1985. Applied Linear Regression. John Wiley, New York. 324 pp.
Wigley, T.M.L., Briffa, K.R., Jones, P.D., 1984. On the average value of correlated time series, with applications in dendroclimatology and hydrometeorology. J. Clim. Appl. Meteor. 23, 201–213.
Woodhouse, C.A., Gray, S.T., Meko, D.M., 2006. Updated streamflow reconstructions for the Upper Colorado River Basin. Water Resour. Res. 42 (W05415). http://dx.doi.org/10.1029/2005WR004,455.
Yang, D., Ye, B., Shiklomanov, A., 2004. Discharge characteristics and changes over the Ob River watershed in Siberia. J. Hydrometeorol. 5, 595–610.